CHAPTER 35

NONLINEAR EVOLUTION OF DIRECTIONAL WAVE SPECTRA IN SHALLOW WATER

Okey Nwogu[1]

ABSTRACT

Nonlinear aspects of the transformation of a multidirectional wave field in shallow water are investigated using Boussinesq-type equations. Second-order interactions between different frequency components in an irregular sca state produce lower and higher harmonic components at the sum and difference frequencies of the primary waves. For water of constant depth, expressions are derived from the Boussinesq equations for the magnitude of the second-order waves induced by bidirectional, bichromatic waves. These are used to investigate the effect of the direction of wave propagation on the near-resonant interactions that occur in shallow water. For waves propagating in water of variable depth, a numerical model based on a time-domain solution of the governing equations is used to the predict the spatial evolution of the directional wave spectrum. The results of the numerical model are compared to experimental results for the propagation of bidirectional, bichromatic waves and irregular, multidirectional waves on a constant slope beach.

1. INTRODUCTION

Surface waves in the occan are short-crested or multidirectional with components of different amplitudes and frequencies, propagating in different directions. As surface waves propagate from deep to shallow water, the directional wave spectrum is transformed due to both linear and nonlinear processes. Linear refraction leads to a narrower directional distribution in shallow water, with the principal direction more closely aligned to the beach contours. Changes to the directional spectrum due to linear effects can be accurately predicted by linear refraction models (e.g. Longuet-Higgins, 1957). However, Freilich *et al.* (1990) found that linear theory could not predict the amplitudes and directions observed in certain frequency bands in field studies. This is due to the near-resonant amplification of wave components induced at the sum and difference frequencies of the primary waves. These wave harmonics could also propagate in directions quite different from those of the primary waves, resulting in substantial changes to the frequency and directional distribution of wave energy.

---

[1] Institute for Marine Dynamics, National Research Council, Ottawa, Canada K1A 0R6

In shallow water depths, Boussinesq-type equations (e.g. Peregrine, 1967) are able to describe the near-resonant quadratic interactions that occur in shoaling multidirectional waves. Various time and frequency domain methods have been used to solve the two-dimensional form of the Boussinesq equations. Liu *et al.* (1985) developed a parabolic model for the shoreward propagation of individual wave components while Kirby (1990) proposed an angular spectrum model. Abreu *et al.* (1992) developed a shallow water spectral model in which near-resonant interactions were only considered between colinear waves. In intermediate water depths, third-order interactions become the dominant nonlinear mechanism for the cross-spectral transfer of energy. Suh *et al.* (1990) have developed an angular spectrum model of the mild-slope equation for Stokes waves which includes cubic interactions.

In this paper, the Boussinesq model of Nwogu (1993) is used to investigate the effect of near-resonant nonlinear wave-wave interactions on the transformation of directional wave spectra in shallow water. Compared to the Boussinesq model of Peregrine (1967), the model proposed by Nwogu (1993) can be applied over a wider range of water depths due to improved frequency dispersion characteristics obtained by changing the velocity variable from the depth-averaged velocity to the velocity at an arbitrary distance from the still water level. Analytical expressions are derived from the Boussinesq equations for the bidirectional quadratic transfer function of the second-order waves induced in water of constant depth. These are used to evaluate the effect of the direction of propagation of the wave components on the near-resonant quadratic interactions that occur in shallow water. For irregular multidirectional waves propagating in water of variable depth, a numerical model based on a time domain solution of the equations is used to predict the spatial evolution of the directional wave spectrum. The results of the numerical model are compared to experimental results for the shoaling of multidirectional waves on a constant slope beach.

2. THEORETICAL MODEL

2.1 Governing Equations

Boussinesq equations represent the depth-integrated equations for the conservation of mass and momentum for weakly nonlinear and mildly dispersive waves, propagating in water of variable depth. By assuming a quadratic variation of the velocity potential over depth, the governing equations of fluid motion can be integrated over the depth, reducing the three-dimensional problem to a two-dimensional one. The continuity and momentum equations can be expressed in terms of the water surface elevation, $\eta(\mathbf{x}, t)$, and the horizontal velocity, $\mathbf{u}_\alpha(\mathbf{x}, t)$, at an arbitrary distance z_α from the still water level as (see Nwogu, 1993):

$$\eta_t + \nabla \cdot [(h + \eta)\mathbf{u}_\alpha] +$$
$$\nabla \cdot \left[\left(\frac{z_\alpha^2}{2} - \frac{h^2}{6} \right) h\nabla(\nabla \cdot \mathbf{u}_\alpha) + \left(z_\alpha + \frac{h}{2} \right) h\nabla[\nabla \cdot (h\mathbf{u}_\alpha)] \right] = 0 \quad (1)$$

$$\mathbf{u}_{\alpha t} + g\nabla\eta + (\mathbf{u}_\alpha \cdot \nabla)\mathbf{u}_\alpha + \left[\frac{z_\alpha^2}{2}\nabla(\nabla \cdot \mathbf{u}_{\alpha t}) + z_\alpha\nabla[\nabla \cdot (h\mathbf{u}_{\alpha t})]\right] = 0 \qquad (2)$$

where $\nabla = (\partial/\partial x, \partial/\partial y)$, $h(\mathbf{x})$ is the water depth and g is the gravitational acceleration. The elevation of the velocity variable z_α is a free parameter and is chosen to minimize the differences between the linear dispersion characteristics of the Boussinesq model and linear theory. An optimum depth for the velocity variable, $z_\alpha = -0.53h$, gives errors of less than 2% in the phase speed from shallow water depths up to the deep water depth limit.

2.2   Second-Order Forced Waves

As surface waves propagate, the different frequency components interact to produce wave components at the harmonics of the primary wave frequencies. The simplest example of this nonlinear phenomenon is the combination of two wave trains with different frequencies. The nonlinear boundary conditions at the free surface result in the generation of forced waves at the sum and difference frequencies of the primary waves, $\omega_1 \pm \omega_2$. The forced waves are bound or phase-locked to the primary waves or wave groups, and propagate in directions given by the sum and difference of the wavenumber vectors, $\mathbf{k}_1 \pm \mathbf{k}_2$. The magnitude of the forced harmonics can be determined by solving the governing equation of motion, with the free surface boundary condition satisfied at second-order in wave steepness. Starting from the Laplace equation, Dean and Sharma (1981) derived expressions for the magnitude of the forced harmonics for bidirectional, bichromatic waves, i.e. two waves with different frequencies, propagating in different directions. We shall now derive corresponding expressions from the Boussinesq equations. Consider a wave train consisting of two periodic waves with frequencies, ω_1 and ω_2, amplitudes, a_1 and a_2, propagating in directions, θ_1 and θ_2 respectively. The water surface elevation is given by:

$$\eta^{(1)}(\mathbf{x}, t) = a_1 \cos(\mathbf{k}_1 \cdot \mathbf{x} - \omega_1 t) + a_2 \cos(\mathbf{k}_2 \cdot \mathbf{x} - \omega_2 t), \qquad (3)$$

where $\mathbf{k} = (k \cos\theta, k \sin\theta)$. The angle, θ, is defined relative to the positive x axis. The individual waves are assumed to satisfy the first-order or linearized form of the Boussinesq equations, i.e.

$$\eta_t^{(1)} + h\nabla \cdot \mathbf{u}_\alpha^{(1)} + \left(\alpha + \frac{1}{3}\right) h^3 \nabla \cdot \left[\nabla(\nabla \cdot \mathbf{u}_\alpha^{(1)})\right] = 0, \qquad (4)$$

$$\mathbf{u}_{\alpha t}^{(1)} + g\nabla\eta^{(1)} + \alpha h^2 \nabla\left(\nabla \cdot \mathbf{u}_{\alpha t}^{(1)}\right) = 0, \qquad (5)$$

where $\alpha = (z_\alpha/h)^2/2 + (z_\alpha/h)$. The wavenumber, k, is thus related to the wave frequency by the following dispersion relation:

$$\frac{\omega^2}{k^2} = gh\left[\frac{1 - \left(\alpha + \frac{1}{3}\right)(kh)^2}{1 - \alpha(kh)^2}\right] \qquad (6)$$

The first-order horizontal velocities corresponding to the water surface elevation given by equation (3) can be determined from equations (4) and (5) as:

$$u_\alpha^{(1)}(\mathbf{x},t) = \frac{\omega_1}{k_1' h} \cos\theta_1 a_1 \cos(\mathbf{k}_1 \cdot \mathbf{x} - \omega_1 t) + \frac{\omega_2}{k_2' h} \cos\theta_2 a_2 \cos(\mathbf{k}_2 \cdot \mathbf{x} - \omega_2 t), \quad (7)$$

$$v_\alpha^{(1)}(\mathbf{x},t) = \frac{\omega_1}{k_1' h} \sin\theta_1 a_1 \cos(\mathbf{k}_1 \cdot \mathbf{x} - \omega_1 t) + \frac{\omega_2}{k_2' h} \sin\theta_2 a_2 \cos(\mathbf{k}_2 \cdot \mathbf{x} - \omega_2 t), \quad (8)$$

where $k' = k[1 - (\alpha + 1/3)(kh)^2]$. At second-order in wave steepness, the surface elevation and velocities have to satisfy the following set of equations:

$$\eta_t^{(2)} + h\nabla \cdot \mathbf{u}_\alpha^{(2)} + \left(\alpha + \frac{1}{3}\right) h^3 \nabla \cdot \left[\nabla(\nabla \cdot \mathbf{u}_\alpha^{(2)})\right] = -\nabla \cdot \left(\eta^{(1)} \mathbf{u}_\alpha^{(1)}\right) \quad (9)$$

$$\mathbf{u}_{\alpha t}^{(2)} + g\nabla\eta^{(2)} + \alpha h^2 \nabla\left(\nabla \cdot \mathbf{u}_{\alpha t}^{(2)}\right) = -\left(\mathbf{u}_\alpha^{(1)} \cdot \nabla\right)\mathbf{u}_\alpha^{(1)} \quad (10)$$

The second-order wave will consist of a sub-harmonic at the difference frequency, $\omega_1 - \omega_2$, and super-harmonics at the sum frequencies, $2\omega_1$, $2\omega_2$ and $\omega_1 + \omega_2$. It can be written as:

$$\begin{aligned}
\eta^{(2)}(\mathbf{x},t) &= \frac{a_1^2}{2} G_+(\omega_1, \omega_1, \theta_1, \theta_1) \cos(2\mathbf{k}_1 \cdot \mathbf{x} - 2\omega_1 t) \\
&+ \frac{a_2^2}{2} G_+(\omega_2, \omega_2, \theta_2, \theta_2) \cos(2\mathbf{k}_2 \cdot \mathbf{x} - 2\omega_2 t) \\
&+ a_1 a_2 G_\pm(\omega_1, \omega_2, \theta_1, \theta_2) \cos(\mathbf{k}_\pm \cdot \mathbf{x} - \omega_\pm t),
\end{aligned} \quad (11)$$

where $\mathbf{k}_\pm = \mathbf{k}_1 \pm \mathbf{k}_2$, and $G_\pm(\omega_1, \omega_2, \theta_1, \theta_2)$ is a bidirectional quadratic transfer function that relates the amplitude of the second-order forced wave to the first-order amplitudes. The quadratic transfer function can be determined by substituting equations (3), (7) and (8) for the first-order surface elevation and velocities into the second-order equations (9) and (10), and solving for the amplitudes of the second-order surface elevation and velocities. This leads to:

$$G_\pm(\omega_1, \omega_2, \theta_1, \theta_2) = \frac{\omega_1 \omega_2 (k_\pm h)^2 \cos\Delta\theta [1 - (\alpha + \frac{1}{3})(k_\pm h)^2]}{2\lambda k_1' k_2' h^3} +$$

$$\frac{\omega_\pm [1 - \alpha(k_\pm h)^2][\omega_1 k_2' h[k_1 h \pm k_2 h \cos\Delta\theta] + \omega_2 k_1' h[k_1 h \cos\Delta\theta \pm k_2 h]]}{2\lambda k_1' k_2' h^3}, (12)$$

where $\Delta\theta = \theta_1 - \theta_2$,

$$k_\pm = |\mathbf{k}_1 \pm \mathbf{k}_2| = \sqrt{k_1^2 + k_2^2 \pm 2k_1 k_2 \cos\Delta\theta}, \quad (13)$$

and

$$\lambda = \omega_\pm^2[1 - \alpha(k_\pm h)^2] - gk_\pm^2 h[1 - (\alpha + 1/3)(k_\pm h)^2]. \quad (14)$$
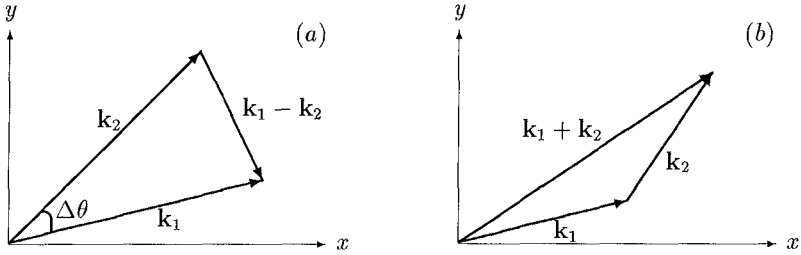
Figure 1. Directions of the sum and difference of the wavenumber vectors.

$\lambda = 0$ is actually the dispersion relation for first-order free waves in the Boussinesq model (Eqn. 6). The second-order forced waves do not satisfy the linear dispersion relation because of the forcing terms on the right hand side of equations (9) and (10), unlike second-order free waves that satisfy the homogeneous part of the equations. The second-order interactions could be resonant ($\lambda \to 0$) if the frequency and wavenumber of the forced wave corresponds to that of a free wave. This occurs to unidirectional wave trains in shallow water depths where the phase velocities of the forced waves are nearly equal to the phase velocities of free waves, leading to a near-resonant amplification of the second-order waves. Wave breaking and cross-spectral energy transfers, however, limit the amplitude of the second-order waves in shallow water.

We shall now examine in detail, the differences between the magnitudes and directions of propagation of the sub-harmonics and super-harmonics in unidirectional and bidirectional seas. The sub-harmonic component, which is commonly referred to as the set-down component, travels at the velocity of the wave group, ω_-/k_-, along a direction defined by the difference of the wavenumber vectors as shown in Figure 1(a). This direction could be quite different from the direction of propagation of the primary waves. If k_1 is nearly equal to k_2, the second-order long wave would travel in a direction almost perpendicular to the average direction of the first-order short waves. On a sloping beach, this might excite the edge (transverse) wave modes as discussed by Gallagher (1971). In contrast, the super-harmonics travel in a direction nearly coincident with the average direction of the primary waves as shown in Figure 1(b).

The quadratic transfer function was evaluated for bidirectional waves with different angles of separation between the individual wave components. The transfer function of the sub-harmonic wave component is plotted in Figure 2 for an example where the frequency difference, $\Delta\omega/\omega = 0.1$, with $\omega_1 = \omega - \Delta\omega/2$ and $\omega_2 = \omega + \Delta\omega/2$. Three crossing angles, $\Delta\theta = 0°$, $10°$ and $20°$ were considered. Also shown in Figure 2 are results obtained from expressions based on a second-order solution of the Laplace equation, derived by Dean and Sharma (1981).

A number of interesting observations can be made from Figure 2. The first one is that for unidirectional waves, the Boussinesq model underestimates the magnitude of the set-down wave, particularly in intermediate water depths. However, for bidirectional
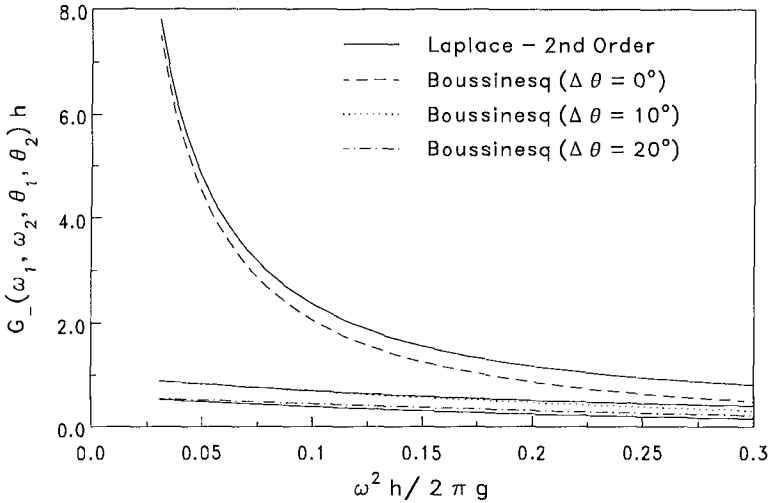
Figure 2. Bidirectional quadratic transfer function for the sub-harmonic component ($\Delta\omega/\omega = 0.1$).

waves, the differences between the Boussinesq and Laplace models becomes negligible. The second one is that the directionality of the waves leads to a significant reduction of the set-down wave, as was noted by Sand (1982). In shallow water with $\omega^2 h/2\pi g < 0.05$, the amplitude of the forced long wave for $\Delta\theta = 10°$ is reduced by at least a factor of 5. This is because forced long waves in directional wave fields are not resonantly amplified in shallow water. Near-resonant amplification occurs for uni-directional waves because the wavenumber of the forced long wave $|k_1 - k_2|$ is nearly equal to that of a free long wave $k(\omega_-)$, or equivalently, ω_- and $|k_1 - k_2|$ nearly satisfy the linear dispersion relation with $\lambda \to 0$ in equation (12). In bidirectional seas, the magnitude of the wavenumber vector of the forced long wave, $|k_1 - k_2|$, is significantly larger than that of the corresponding free wave $k(\omega_-)$ for small angles of separation. The forced waves are, thus, no longer close to satisfying the dispersion relation for free waves.

The quadratic transfer function for the super-harmonics is plotted in Figure 3 for an example with $\Delta\omega/\omega = 0.1$, and $\Delta\theta = 0°$ and $40°$. The forced higher harmonics are slightly reduced in bidirectional waves, but not as significantly as the sub-harmonic component. For $\omega^2 h/2\pi g = 0.05$ and $\Delta\theta = 20°$, the super-harmonic component is reduced by 12%, compared to 90% for the sub-harmonic component. In contrast to the sub-harmonics, the super-harmonics in directional wave fields are resonantly amplified in shallow water. This is because with the addition of the wavenumber vectors, the magnitude of of the wavenumber vector of the forced super-harmonic is closer to that of the corresponding free wave. The directional wave transformation model proposed
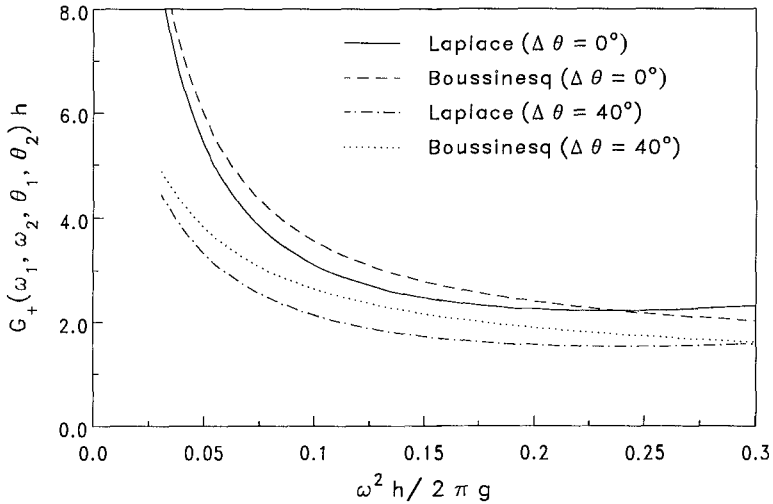
Figure 3. Bidirectional quadratic transfer function for the super-harmonic component ($\Delta\omega/\omega = 0.1$).

by Abreu *et al.* (1992) assumes that near-resonant, second-order interactions only occur between colinear waves in shallow water. The present analysis, does, however, show that second-order interactions between non-colinear waves in shallow water are near-resonant for the super-harmonic component, although the strength of the interaction decreases with increasing angular separation.

3. Time Domain Solution

For waves propagating in water of variable depth, free second and higher-order waves are generated in addition to the forced waves. The bidirectional quadratic transfer function (Eqn. 12) can no longer be used to determine the amplitude of the wave harmonics. In this paper, we employ the time-domain model of Nwogu (1995) for irregular multidirectional wave propagation in water of variable depth. The model solves the governing set of Boussinesq-type equations using an iterative Crank-Nicolson finite difference method, with a predictor-corrector scheme used to provide the initial estimate. The computational domain is discretized using a rectangular grid, with the dependent variables η, u_α and v_α defined at the grid points in a staggered manner. The numerical solution procedure consists of solving an algebraic expression for η at all grid points, tridiagonal matrices for u_α along lines in the x direction and tridiagonal matrices for v_α along lines in the y direction at every time step. Details of the third-order accurate scheme can be found in Nwogu (1995).

The boundaries of the computational domain may be specified as wave input boundaries or solid walls. Along incident wave boundaries, time series of u_α, $u_{\alpha,xx}$ and $v_{\alpha,xy}$ or v_α, $v_{\alpha,yy}$ and $u_{\alpha,xy}$, corresponding to regular or irregular, unidirectional or multidirectional sea states are input at the grid points. The time histories may be derived from target directional wave spectra using the random phase, single direction per frequency model of wave synthesis (see Miles and Funke, 1987). Waves propagating out of the domain are artificially absorbed in damping regions placed next to solid wall boundaries. Artificial damping of wave energy is accomplished by introducing terms out of phase with the water surface velocity and fluid acceleration into the continuity and momentum equations respectively (see Nwogu, 1995). The output of the numerical model are time histories of η, u_α and v_α at desired grid points in the computational domain. Directional wave spectra estimates are obtained from the time records by using the high resolution, maximum entropy method (Nwogu *et al.*, 1987)

4. NUMERICAL AND EXPERIMENTAL RESULTS

Laboratory experiments were also conducted to investigate the propagation of multidirectional waves on a constant slope beach. The experiments were carried out in the three-dimensional wave basin of the Hydraulics Laboratory, National Research Council of Canada. The basin is 30 m wide, 20 m long and 3 m deep and is equipped with a 60-segment directional wave generator. The individual wave boards are 0.5 m wide and 2 m high. Wave energy absorbers made of perforated metal sheets are installed along the other sides of the basin not occupied by the wave generator. A 1:25 constant slope beach with an impermeable concrete cover was constructed in the basin, parallel to the wave generator. The toe of the slope was located 4.6 m away from the wave boards. Bidirectional bichromatic waves and irregular multidirectional sea states were generated in the basin. The water depth in the constant depth portion of the basin was 0.56 m. The water surface elevation along the centerline of the basin was measured with a linear array of 23 water level gauges. The experimental set-up is discussed in greater detail in Nwogu (1993).

4.1   Shoaling of Bidirectional, Bichromatic Waves

Consider the shoaling of a bichromatic wave train with component wave periods, $T_1 = 1.65$ s, $T_2 = 1.5$ s, and heights, $H_1 = 0.041$ m, $H_2 = 0.037$ m. The tests were carried for both a unidirectional version with $\theta_1 = \theta_2 = 0°$, and a bidirectional version with $\theta_1 = 30°$ and $\theta_2 = -15°$. The spectral density of the measured surface elevation time history at location ($h = 0.134$ m) is shown in Figure 4 for the bidirectional wave train. In addition to second-order wave harmonics at $2f_1$, $2f_2$ and $f_1 \pm f_2$, third-order wave components are also observed at $2f_1 \pm f_2$, $2f_2 \pm f_1$, $3f_1$, and $3f_2$, as well as some fourth-order components.

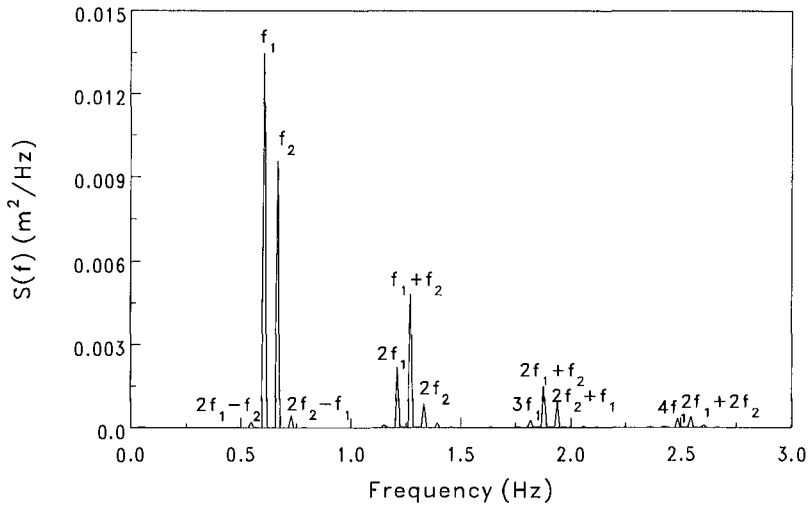The numerical model was used to simulate the propagation of the unidirectional and

Figure 4. Measured spectral density in shallow water for a bidirectional bichromatic wave train ($\Delta\theta = 45°$, $h = 0.134$ m).

bidirectional wave trains on the 1:25 beach. The simulations were carried out using a time step size $\Delta t = 0.05$ s, and spatial grid sizes $\Delta x = 0.1$ m and $\Delta y = 0.2$ m. A contour plot of the instantaneous water surface elevation in the basin for the bidirectional wave train is shown in Figure 5. The variation in amplitude of a select number of wave harmonics along the centerline of the basin are plotted in Figure 6 for the unidirectional wave train, and Figure 7 for the bidirectional wave train. The experimental results are also shown in the figures. The Boussinesq model is observed to reasonably predict the measured variation in amplitude of the first-order waves and higher harmonics. The model, however, underestimates the magnitude of the set-down component for the unidirectional wave in shallow water. The simulated set-down wave has an amplitude of 0.003 m at $h = 0.134$ m, while the measured wave has an amplitude of 0.006 m. The numerical model underestimates the magnitude of the long period wave partly because it does not simulate the reflected free waves that are generated after wave breaking and runup.

The ability of the numerical model to predict the change in wave direction between the deep and shallow water depths was also examined. The maximum entropy method, described by Nwogu et al. (1987), was used to estimate the directional distributions at different frequency bands from the simulated η, u_α and v_α time series. The directions in the deep ($h = 0.56$ m) portion of the basin are $\theta(f_1) = 30°$ and $\theta(f_2) = -15°$. At $h = 0.134$ m, the Boussinesq model predicts $\theta(f_1) = 18°$ and $\theta(f_2) = -13°$ while Snell's law predicts $\theta(f_1) = 27°$ and $\theta(f_2) = -13°$. Good agreement is observed for the $-15°$ wave but not the $30°$ wave. The differences are primarily due to diffraction
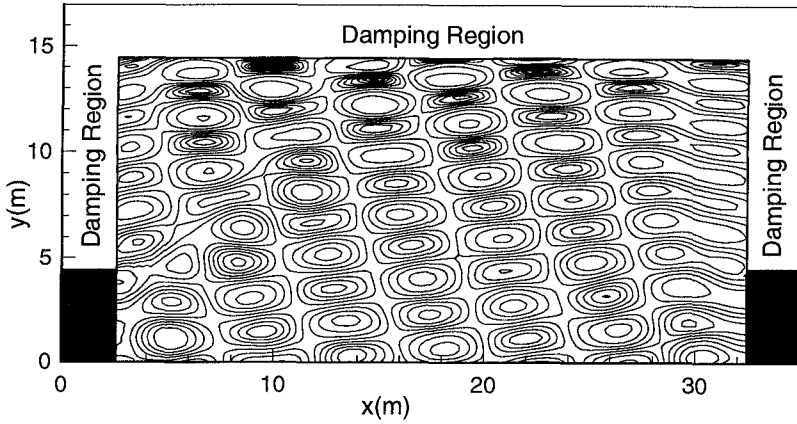
Figure 5. Contour plot of instantaneous water surface elevation for a bidirectional bichromatic wave train shoaling on a 1:25 beach ($\theta_1 = 30°$, $\theta_2 = -15°$).
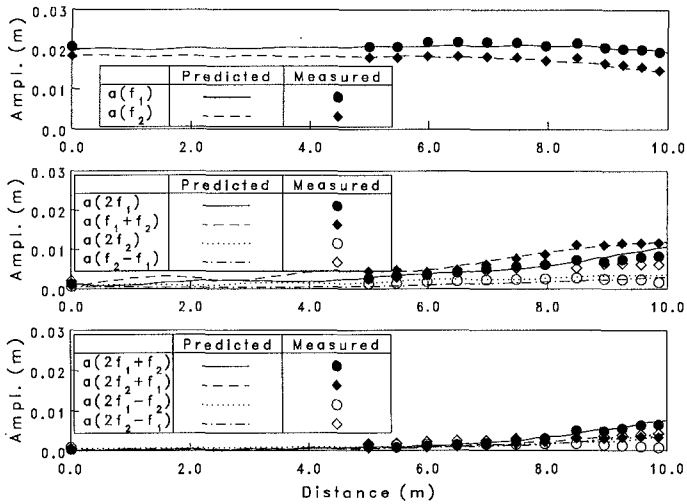

Figure 6. Variation in amplitude of wave harmonics for a unidirectional bichromatic wave train shoaling on a 1:25 beach ($\Delta\theta = 0°$).
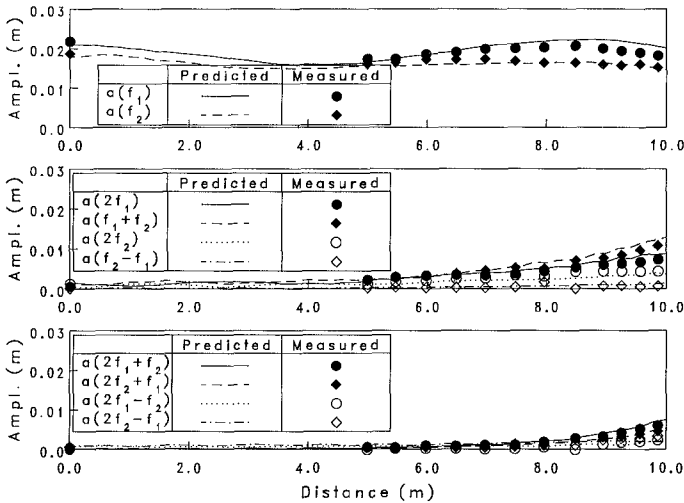
Figure 7. Variation in amplitude of wave harmonics for a bidirectional bichromatic wave train shoaling on a 1:25 beach ($\Delta\theta = 45°$).

effects caused by the finite width of the wave generator. The effect of diffraction is more important in the shallow portion of the basin for oblique waves with large angles of incidence. For the second-order higher harmonics, the numerical model predicts $\theta(2f_1) = 19°$, $\theta(f_1 + f_2) = 2°$, and $\theta(2f_2) = -12°$. The predicted direction for the sum frequency component is within 2° of that determined from the sum of the wavenumber vectors.

4.2 Shoaling of Irregular Multidirectional Waves

Consider the shoaling of a bimodal sea state with local sea and swell components on the 1:25 beach from deep ($h = 0.56$ m) to shallow water ($h = 0.18$ m). The incident sea states were synthesized using the random phase, single direction per frequency model of wave synthesis (see Miles and Funke, 1987). The JONSWAP spectrum was used to describe the frequency distribution of wave energy while the parametric cosine power function was used for the directional distribution. The local sea component has a significant wave height, $H_{mo} = 0.062$ m, peak period, $T_p = 1.5$ s, peak enhancement factor, $\gamma = 3.3$, and a directional distribution defined by $D(\theta) = \cos^{12}(\theta - 22.5°)$. The swell component is characterized by $H_{mo} = 0.068$ m, $T_p = 2$ s, $\gamma = 10$, and $D(\theta) = \cos^{44}(\theta + 22.5°)$. The incident directional wave spectrum is shown in Figure 8.

The Boussinesq model was used to simulate the shoaling of the bimodal sea state with
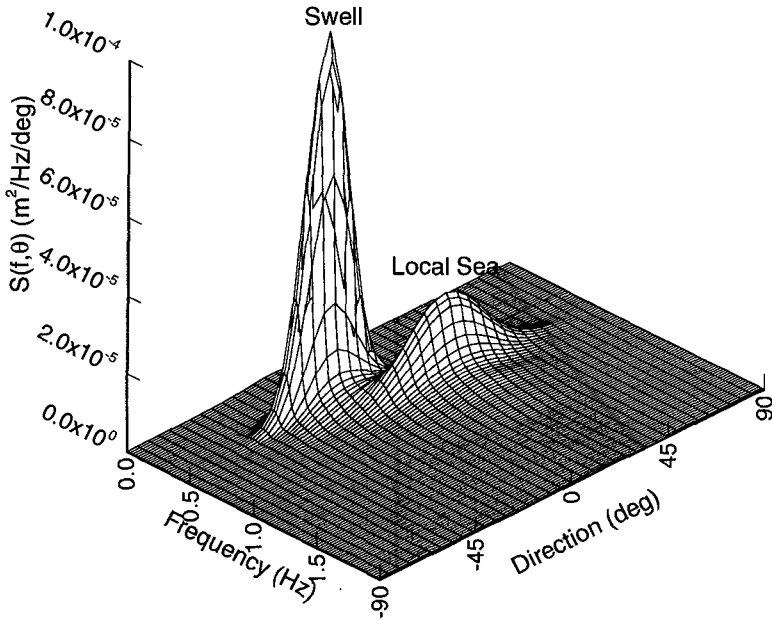
Figure 8. Numerically simulated directional spectrum of a bimodal sea state in deep
        water ($h = 0.56$ m).

time step size, $\Delta t = 0.05$ s and spatial grid sizes, $\Delta x = 0.1$ m, $\Delta y = 0.2$ m. Figure 9 shows a comparison of the wave spectrum at $h = 0.56$ m with the measured and predicted spectral densities at $h = 0.18$m. Reasonably good agreement is observed between the measured and predicted wave spectra. Directional spectral estimates were also obtained from the simulated η, u_α and v_α time histories using the maximum entropy method (Nwogu *et al.*, 1987). The predicted directional spectrum at $h = 0.18$ m is shown in Figure 10. Nonlinear wave-wave interaction effects in the shoaling process substantially change the directional wave spectrum, with the transfer of energy across frequency and direction bands. There is a growth of the second, third and fourth harmonics of the swell component, and the generation of components at the vector sum of the local sea and swell components, and the vector sum of the local sea and second harmonic of the swell component. Such modifications of the directional wave spectrum can only be obtained with the use of a model that simultaneously treats nonlinearity and directionality in shoaling waves.
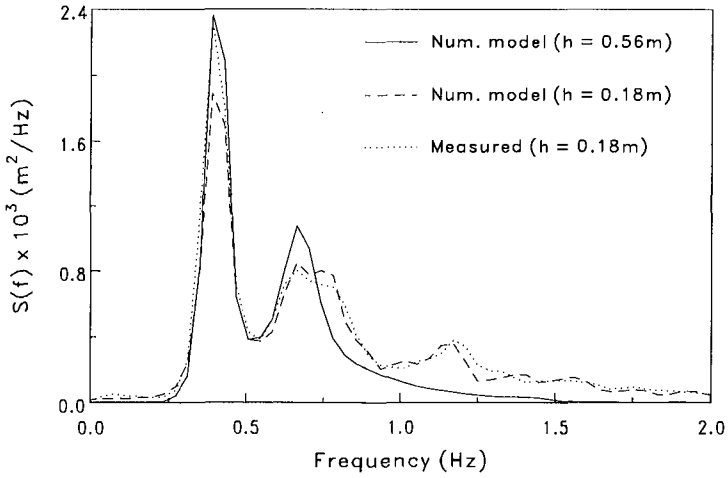
Figure 9. Surface elevation spectral densities at different water depths for bimodal sea state.
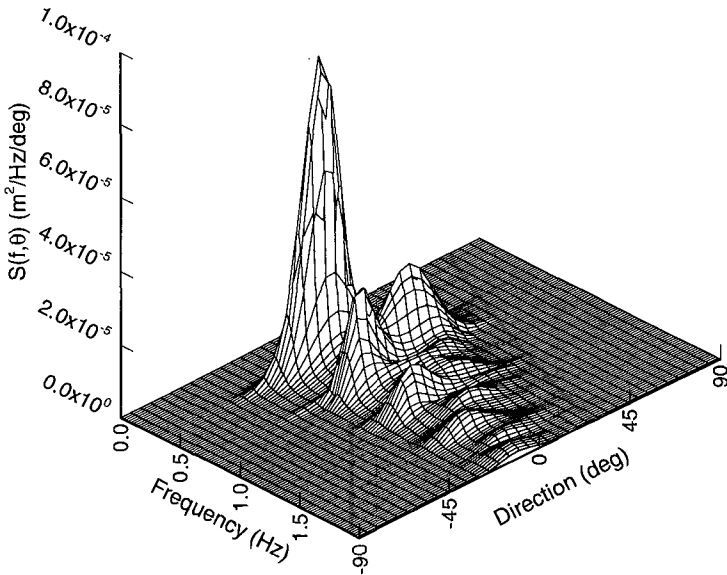

Figure 10. Numerically simulated directional spectrum of a bimodal sea state in shallow water ($h = 0.18$ m).

5. CONCLUSIONS

A Boussinesq model has been used to investigate the effect of near-resonant nonlinear interactions on the transformation of directional wave spectra in shallow water. The amplification of second-order components induced at the sum and difference frequencies of the primary waves is near-resonant for unidirectional waves in shallow water. In multidirectional sea states, however, the second-order interactions are near-resonant for the higher harmonics but non-resonant for the lower harmonics. This leads to a significant reduction in magnitude of the long period waves induced by shoaling multidirectional waves. The spatial evolution of the directional wave spectrum in water of variable depth was predicted using a time domain Boussinesq model, and the maximum entropy method for directional wave analysis. The numerical model, which includes the effects of shoaling, refraction, diffraction and reflection, was able to predict a substantial modification of the directional wave spectrum in shallow water due to near-resonant nonlinear interactions.

REFERENCES

Abreu, M., Larraza, A., and Thornton, E. 1992. Nonlinear transformation of directional wave spectra in shallow water. *Journal of Geophysical Research*, **97**, 15579-15589.

Dean, R.G., and Sharma, J.N. 1981. Simulation of wave systems due to nonlinear directional spectra. *Proc. Int. Symposium on Hydrodynamics in Ocean Engineering*, Trondheim, Norway, 1211-1222.

Freilich, M.H, Guza, R.T., and Elgar, S.L. 1990. Observations of nonlinear effects in directional spectra of shoaling gravity waves. *Journal of Geophysical Research*, **95**, 9645-9656.

Gallagher, B. 1971. Generation of surf beat by non-linear wave interactions. *Journal of Fluid Mechanics*, **49**, 1-20.

Kirby, J.T. 1990. Modelling shoaling directional wave spectra in shallow water. *Proc. 22nd Int. Conference on Coastal Engineering*, Delft, The Netherlands, 109-122.

Liu, P.L.-F., Yoon, S.B., and Kirby, J.T. 1985. Nonlinear refraction-diffraction of waves in shallow water. *Journal of Fluid Mechanics*, **153**, 185-201.

Longuet-Higgins, M.S. 1957. On the transformation of a continuous spectrum by refraction. *Proc. Cambridge Phil. Soc.*, **53**, 226-229.

Miles, M.D., and Funke, E.R. 1987. A comparison of methods for the synthesis of directional seas. *Proc. 6th Int. Offshore Mechanics and Arctic Engineering Symposium*, Houston, II, 247-255.

Nwogu, O. 1993. Alternative form of Boussinesq equations for nearshore wave propagation. *Journal of Waterway, Port, Coastal and Ocean Engineering*, ASCE, **119**(6), 618-638.

Nwogu, O. 1995. Time domain simulation of shoaling multidirectional waves. *submitted to Coastal Engineering*.

Nwogu, O., Mansard, E.P.D., Miles, M.D, and Isaacson, M. 1987. Estimation of directional wave spectra by the maximum entropy method. *Proc. IAHR Seminar on Wave Analysis and Generation in Laboratory Basins*, XXII IAHR Congress, Lausanne, 363-376.

Peregrine, D.H. 1967. Long waves on a beach. *Journal of Fluid Mechanics*, **27**, 815-827.

Sand, S.E. 1982. Long waves in directional seas. *Coastal Engineering*, **6**, 195-208.

Suh, K.D., Dalrymple, R.A., and Kirby, J.T. 1990. An angular spectrum model for propagation of Stokes waves. *Journal of Fluid Mechanics*, **221**, 205-232.